

The vertical motion of particles is considered for a tall vibrating system; a study is made of the effects of stress waves on the distance between the bottom of the vessel and the bottom of the bed.

Vertical vibration of a vessel containing a fine powder may be accompanied by periodic detachment of the layer from the bottom and fluidization by the gas infiltrating from the gap, which, in turn, may be accompanied by gas bubbles, rapid circulation, and extensive mixing of the material.

Kroll [1] first considered the motion and later Yoshida and Kousaka [2]. The layer was represented as a rigid porous body, which gave the path followed by the bed and the parameters of the vibration at which cyclic fluidization was produced by a pulsating gas flow. However, the specification of bed rigidity and the use of a relation for detachment of a heavy material point as the initial condition resulted in formulas that reflect only the motion of shallow layers.

Oscilloscope recordings have been made of the pressure exerted by electrocorundum particles of small size (0.08-1.32 mm) on a membrane built into the bottom [3], and this indicated that rapidly damped vibrations arise when the material strikes the bottom, resulting in a pressure on the bottom in addition to the inertial dynamic pressure.

These vibrations are damped out in the lower layers long before the end of the joint motion of the particles and bottom (Fig. 1). Therefore, they have no effect on the instant of detachment, and the phase angle of detachment can be found from the condition that the compressive forces at the lower boundary of a rigid porous body vanish, which is [4] defined by the following formula that incorporates the dissipation:

$$\sin \theta_0 = \frac{\varphi_v}{K_v}, \quad (1)$$

$$\varphi_v = \frac{\eta H_p}{1 - \exp(-\eta H_p)}. \quad (2)$$

Here φ_v is the coefficient for the delay in the vibrational detachment for an unbounded layer, K_v is the relative acceleration due to the vibration, $\theta_0 = \omega\tau$ is the detachment angle, τ is time, and η is the damping coefficient.

The amplitude and duration of the shock and, consequently, also of the free vibrations increase with the height of the bed, and the power part of the bed has time to perform not more than one oscillation during the time of contact for a height greater than 0.1 m. The total pressure on the bottom at the end of the contact phase may be less than or greater than the inertial pressure, in accordance with the phase of the vibration, and this can delay or accelerate the loss of compressive stresses. Therefore θ_0 does not vary in a monotonic fashion with the height of the bed, although (1) would imply this, but instead passes through a series of turning points. The value of θ_0 approaches the limit of $\pi/2$ near the maxima. Near the minima, the angle falls to values close to or less than the angle of detachment for a heavy material point θ_0^h as given by (1) as $H_p \rightarrow 0$ (Fig. 1). Consequently, the lift-off is not damped for $H_p > 0.2-0.4$ m, as is usually assumed, but persists up to $H_p = 1$ m or more. These turning-point values for the angle occur at smaller bed depths as the vibration frequency increases or the particle size is reduced.

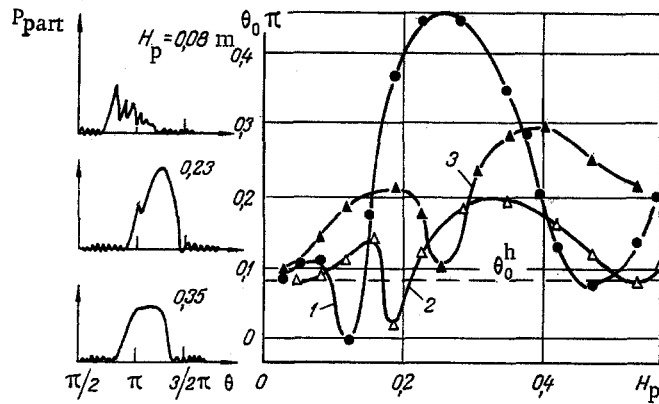


Fig. 1. Oscillograms for the particle pressure p_{part} on the bottom ($d = 0.8$ mm; $f_v = 20$ Hz) and angle of detachment of 0.08-mm-diameter particles at 20 Hz (1); the same for 0.20-mm particles at 20 Hz (2) and 16 Hz (3); $A_v = 2.73$ mm; π , rad.

We have determined the conditions under which the dynamic stresses at the bottom and the angles of detachment for deep beds ($H_p > 0.1$ m) attain their turning-point values by considering the equivalent problem of the propagation of quasielastic waves in an imperfectly elastic porous body whose center of mass is at rest in the coordinate system. To avoid complications we assume that the transverse dimensions of the apparatus are fairly large ($D > 0.1$ m from the data of [5]), which means that the friction between the material and the wall can be neglected. Then the motion is described by

$$\frac{\partial^2 \vartheta_d}{\partial \tau^2} = C_v^2 \frac{\partial^2 \vartheta_d}{\partial z^2} + \varphi. \quad (3)$$

Here C_v is the speed at which the dynamic stresses propagate from the vibration source along the bed skeleton, while $\vartheta_d(z, \tau)$ is the displacement of an arbitrary section of the body relative to the center of mass and $\varphi = \varphi_1 + \varphi_2$ corrects for the loss of momentum.

The dynamic stresses are dissipated as they propagate through the bed, the dissipation being proportional to the relative strain rate $\partial \vartheta_d / \partial z$:

$$\sigma_{z_1} = \rho_d v_d \frac{\partial^2 \vartheta_d}{\partial z \partial \tau}, \quad (4)$$

where v_d is a coefficient representing the effective viscosity; then $\varphi_1(z, \tau)$, which incorporates the dissipation of the momentum on account of the imperfect elasticity, is

$$\varphi_1(z, \tau) = \frac{1}{\rho_d} \cdot \frac{\partial \sigma_{z_1}}{\partial z} = v_d \frac{\partial^3 \vartheta_d}{\partial z^2 \partial \tau}. \quad (5)$$

The function $\varphi_2(z, \tau)$ incorporates the damping action of the gas moving in the pores; it differs from zero if the pores are small and the speed of the powder differs from that of the gas. The value of φ_2 for small particles is defined by the linear part of Ergun's formula:

$$\varphi_2(z, \tau) = -\frac{1}{\rho_d} \cdot \frac{\partial p}{\partial z} = F \Delta W = F \frac{\partial}{\partial \tau} (\vartheta - \vartheta_d), \quad (6)$$

where $F = 150[(1 - \epsilon)/\epsilon^3] \cdot [\mu_c / \rho_M (\varphi_M d)^2]$ and ΔW is the flow speed of the fluid relative to the skeleton after ejection from the gaps between the particles.

The displacement of the gas ϑ in the pores arises from variation in the velocity; so the speed $\partial \vartheta / \partial \tau$ will be related as follows ([6], p. 387) to the speed of the skeleton:

$$\epsilon \frac{\partial \vartheta_d}{\partial \tau} = -(1 - \epsilon) \frac{\partial \vartheta_d}{\partial \tau}. \quad (7)$$

From (4)-(7) we have that the equation of motion is

$$\frac{\partial^2 \vartheta_d}{\partial \tau^2} = C_v \frac{\partial^2 \vartheta_d}{\partial z^2} + v_d \frac{\partial^2 \vartheta_d}{\partial z \partial \tau} - F \frac{\partial \vartheta_d}{\partial \tau} \quad (8)$$

A regular periodic deformation is applied to the lower boundary of the model, which is harmonic to a first approximation:

$$\vartheta_d(0, \tau) = \vartheta_{d,0} \sin \omega \tau, \quad (9)$$

where $\vartheta_{d,0}$ is the amplitude of the strain.

Then a damped wave of the following form propagates in the body [7]:

$$\vartheta_{d1} = \vartheta_{d,0} \exp(-\eta z) \cos(\omega \tau - \chi z). \quad (10)$$

The incident wave is reflected downwards as a relaxation wave at the upper free boundary:

$$\vartheta_{d2} = a \vartheta_{d,0} \exp[-\eta(2H_p - z)] \cos[\omega \tau - \chi(2H_p - z)], \quad (11)$$

$$\eta^2 = \frac{k^2}{2} \left\{ \frac{m(n-m)}{1-m^2} - 1 + \sqrt{\left[1 - \frac{m(n-m)}{1-m^2} \right]^2 + \frac{(n-m)^2}{(1-m^2)^2}} \right\}, \quad (12)$$

$$\chi^2 = \frac{k^2}{2} \left\{ 1 - \frac{m(n-m)}{1-m^2} + \sqrt{\left[1 - \frac{m(n-m)}{1-m^2} \right]^2 + \frac{(n-m)^2}{(1-m^2)^2}} \right\}, \quad (13)$$

where $\eta \geq 0$ is the damping coefficient, a is the reflection coefficient, and χ is the analog of the wave number $k = \omega/C_v$ for the phase velocity $C_{ph} = \omega/\chi$. Then $\chi = k$ and $n = F/\omega$ is a dimensionless parameter representing the ratio of the viscous forces of the gas to the inertial forces of the skeleton in the absence of dissipation. This determines the rate of dissipation of the momentum transferred to the material by the bottom and the reduction in the path traveled by the wavefront during the period of vibration. In the limit $n \rightarrow \infty$, the energy is dissipated in a layer of infinitely small height, while the wavelength of the perturbation and the phase velocity tend to zero.

On the other hand, the dimensionless parameter $m = v_d \chi^2 / 4\pi^2 \omega$ represents the increase in the rigidity of the material by comparison with that of an ideally elastic body ($v_d = 0$) and as a consequence implies an increase in the signal velocity and in the height traveled during the vibration period.

The condition for a turning point in the dynamic stress at the bottom can be determined by considering only the first reflected wave, since the subsequent ones will only accentuate or attenuate the amplitude of the resultant stresses without effect on the phase. Then the relative motion in the material is determined by the form of the signal arising from the interaction of two waves: consolidation and expansion $\vartheta_d = \vartheta_{d1} + \vartheta_{d2}$, and this is dependent on the phase shift between the forward and reflected waves.

The rate of the relative strain $\partial^2 \vartheta_d / \partial z \partial \tau$ in a powder containing a gas is less than that for an evacuated powder $\partial^2 \vartheta_d' / \partial z \partial \tau$ having the effective modulus of elasticity $E_v [\partial \vartheta_d / \partial z = (1/E_v) \sigma_z]$ by an amount dependent on the viscous forces arising from the infiltration:

$$\partial^2 \vartheta_d'' / \partial z \partial \tau = -F \sigma_z.$$

The relationship between the relative deformation and the dynamic stresses is of the form

$$\frac{\partial^2 \vartheta_d}{\partial z \partial \tau} = \frac{\partial^2 \vartheta_d'}{\partial z \partial \tau} + \frac{\partial^2 \vartheta_d''}{\partial z \partial \tau} = \frac{1}{E_v} \frac{\partial \sigma_z}{\partial \tau} - F \sigma_z. \quad (14)$$

We solve (14) for σ_z to get

$$\sigma_z(z, \tau) = e^{\int_0^\tau F d\tau} E_v \int_0^\tau \frac{\partial^2 \vartheta_d}{\partial z \partial \tau} e^{-\int_0^\tau F d\tau} d\tau, \quad (15)$$

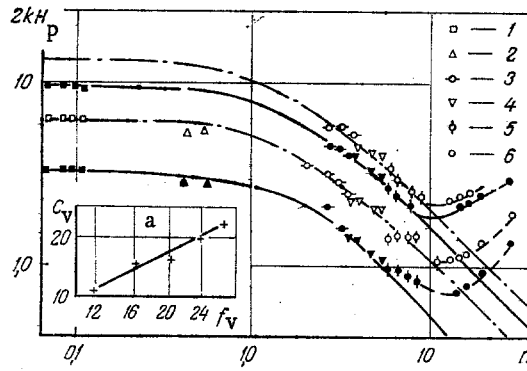


Fig. 2. Dimensionless bed height giving maximum angle of detachment (solid line, filled points), and minimum angle (dashed-dot line, open points) in terms of the dimensionless hydraulic-resistance coefficient for corundum powder for $H_d \leq 0.7$ m in a vessel of diameter 0.1-0.3 m for a vibration amplitude of 2.73 mm; a) empirical relationship for the phase velocity C_v (mm/sec) as a function of vibrational frequency f_v in Hz: 1) $d = 1.32$ mm; 2) 0.5; 3) 0.2; 4) 0.16; 5) 0.12; 6) 0.08 mm.

where $\partial^2 \theta_d / \partial z \partial \tau = \partial^2 / \partial z \partial \tau (\theta_{d1} + \theta_{d2})$ is a complex sign-varying function of the height and frequency; the pressure on the bottom may actually decrease as the height of the bed increases; the condition for σ_z at the lower boundary to have a turning point takes the form

$$\sin [(\chi' - 1)N + \psi] \exp(-Nn) + A \sin(\chi'N) = 0, \quad (16)$$

$$N = 2H_p \chi; \quad \chi' = \frac{\chi}{k}; \quad \psi = \arctg n; \quad A = \sqrt{\frac{1+n^4}{1+n^2}}. \quad (17)$$

In deriving (16) we have incorporated the fact that the time needed for the signal to propagate to the upper boundary and back again is $\tau = 2H_p / C_{ph}$; (16) as $n \rightarrow 0$ ($n < 0.1$) is the standard condition for resonance in an elastic rod: $\sin 2kH_p = 0$, whereas the exponential factor falls to zero for $n > 2-3$ and the turning-point condition simplifies to

$$\sin \chi'N = 0. \quad (18)$$

There is a minor discrepancy between the exact formula (16) and the approximate one (18) in the region $0.1 < n < 1.5$, but this does not exceed 5-7%.

The roots of (18) are multiples of π : $\chi'N = i\pi$; $i = 1, 2, \dots$; we determine the sign of the second derivative $\partial^2 \sigma_z / \partial z^2$ at the turning points to establish that the dynamic stresses on the bottom are maximal for i even, whereas they are minimal for i odd. A change from one to the other occurs on increasing the height of the bed by $\delta H_p = 0.5\pi k / \chi^2$.

Calculations from (15)-(18) show that coarse powders ($n < 0.1$) give minimal dynamic stresses on the bottom that are always positive.

The minimum dynamic stresses decrease as n increases, and they become negative for $n > 0.25$; then the total stress on the bottom during the period of contact will be less than the quasistationary stress arising from the vibrational inertia, and the material will detach from the bottom earlier than the classical theory for a rigid porous body would imply, as is confirmed by the measurements of Fig. 1, where θ_0 for curves 1 and 2 with $H_p = 0.12$ and 0.18 m is less than θ_0^h .

Figure 2 shows results from (18) in the form of dimensionless height $2kH_p$ as a function of $n = F/\omega$ for i of 1-4; we also show the observed values for the dimensionless bed height at which the detachment angles are minimal (open points) and maximal (filled points). The ordinate points were determined via the following identity: $2kH_p = i\pi(H_f/H_v)^2$, where H_f and H_v are the measured heights for finely divided material ($n > 0.1$) and coarse material ($n < 0.1$), respectively, at which the detachment angles are extremal. The value for C_v was selected during the processing, and since it appears in $2kH_p (C_v = \omega/k)$, was found to be proportional to the square root of the vibrational frequency (Fig. 2a), but it was not dependent on the particle size. The increase in C_v in the model body is due to the increase in the effective

rigidity of the elastoviscous skeleton on increasing the vibrational frequency. This model gives a good qualitative description of the motion and a reasonably complete quantitative description for $n < 5-10$; quantitative discrepancies occur for $n > 10$ on account of the gas compressibility, and Kroll has shown that this becomes more pronounced as the particle size decreases, while the model also becomes less strictly applicable.

NOTATION

A_v , vibration amplitude; d , particle diameter; f_v , vibration frequency; g , acceleration of gravity; H_p , height of dense bed; p , gas pressure; z , vertical coordinate; ϵ , porosity; μ_c , ν_c , dynamic and kinematic viscosities of gas; ρ_M , ρ_d , densities of material and of dense bed; σ_z , normal vertical stresses; Φ_M , particle shape factor; ω , angular frequency.

LITERATURE CITED

1. W. Kroll, *Forsch. Gebiete Ing.*, 20, No. 1, 2-15 (1954).
2. T. Yoshida and I. Kousaka, *Chem. Eng., Japan*, 5, No. 1, 159-163 (1967).
3. A. F. Ryzhkov, in: *Industrial Fluidized-Bed Ovens [in Russian]*, Izd. UPI, Sverdlovsk (1973), p. 12.
4. A. F. Ryzhkov and A. P. Baskakov, *Teor. Osnovy Khim. Tekhnol.*, 8, No. 6 (1974).
5. A. F. Ryzhkov, Author's Abstract of Candidate's Dissertation, Ural Polytechnic Institute, Sverdlovsk (1974).
6. S. Sou, *Hydrodynamics of Multiphase Systems [Russian translation]*, Mir, Moscow (1971).
7. H. Kolsky, *Stress Waves in Solids*, Dover (1963).

EQUATIONS FOR THE HEAT FLUXES IN THE CATHODE AND ANODE SECTIONS OF A TWO-JET PLASMA SOURCE

S. P. Polyakov and M. G. Rozenberg

UDC 533.9.07

General relationships are derived for the heat fluxes at the cathode, anode, and nozzles of a two-jet plasma source working with air at atmospheric pressure.

A two-jet plasma source is an economical form of high-temperature open-arc source; engineering calculations require general relationships for volt-ampere characteristics, thermal efficiency, and heat fluxes at the electrodes. Equations for the voltages, currents, and efficiency have been given [1] for air at atmospheric pressure, but no values were given for the heat fluxes at the electrodes. These are very important, since a knowledge of these fluxes in terms of the other parameters is required in order to design a system with a higher thermal efficiency and better erosion resistance in the electrodes and nozzles.

The present study is a continuation of [1] and deals with the heat fluxes in the electrodes in such a source working in air at atmospheric pressure.

The apparatus, the arc-striking system, and the working parameters have previously been given [1]; the power supply was a dc source with an open-circuit voltage of 600 V. The arc current was varied over the range 80-250 A, while the power drawn did not exceed 90 kW. The air flow rate in each electrode unit varied over the range $0.3-1.5 \cdot 10^{-3}$ kg/sec.

The electrical parameters and the heat fluxes to the electrodes and nozzle were measured; the temperature of the cooling water was measured with a precalibrated differentiated six-junction Chromel-Copel thermocouple. The emfs were recorded with an N-700 loop oscilloscope. The water flow rate was measured with rotameters and measuring vessels. The error in determining the heat fluxes did not exceed $\pm 15\%$.